Feasibility of a MEMS Sensor for Gas Detection in HV Oil-Insulated Transformer

Krishna Prasad Bhat, *Member, IEEE*, Kwang W. Oh, and
Douglas C. Hopkins, *Senior Member, IEEE*

***Abstract*—This paper addresses protection of oil-insulated transformers, using a microelectromechanical systems (MEMS) sensor system to augment or replace existing protection techniques. Traditional technologies used for protection and analysis involve pressure and temperature sensing, gas chromatography, and/or a Buchholz relay. The proposed MEMS device is immersed within the insulating fluid, e.g., oil, and primarily consists of multiple microscale turbines centrally shafted to a MEMS generator. The device utilizes relative differences in the velocity, pressure, and flow rate of fluid caused by electric faults. A differential electrical output is produced, which can be coupled to a remote recorder.**

***Index Terms*—Fault diagnosis, fluid flow measurement, fluidic microsystems, gas detectors, microelectromechanical systems (MEMS), oil insulation, power transformers.**

NOMENCLATURE

$\Delta\Phi$	Minimum work done.
P_o	Ambient (nucleation) pressure.
P	Pressure of gas bubble.
R	Radius of gas bubble.
K	Boltzmann's constant.
T	Temperature of gas bubble.
σ	Surface tension of fluid interface.
n_i	Number of molecules of component in a vapor mixture.
y/y_i	Volume fraction.
dE	Total energy of the layer.
dE_1	Potential energy of the gas.
dE_2	The kinetic energy of the layer.
dE_3	The energy due to surface tension.
φ	Gas volume fraction.
Q_g	Volumetric flow rate of gas.
ρ_f; ρ	Density of fluid.
ρ_g	Density of gas.
v_f	Velocity of fluid interface.
x	Distance traveled by the interface.
c_i; c_j	Molecular velocity vectors.
F_i	Force per unit mass.
τ	Energy flux.
q_i	Heat flux.
h	Enthalpy.
e	Energy per unit mass.
M	Torque developed.

Manuscript received March 19, 2011; revised May 8, 2012; accepted May 18, 2012. Date of publication November 22, 2012; date of current version January 16, 2013. Paper 2010-EPC-429.R1, presented at the 2010 Industry Applications Society Annual Meeting, Houston, TX, October 3–7, and approved for publication in the IEEE TRANSACTIONS ON INDUSTRY APPLICATIONS by the Electrostatic Processes Committee of the IEEE Industry Applications Society.

K. P. Bhat and K. W. Oh are with the Department of Electrical Engineering, University at Buffalo, State University of New York, Buffalo, NY 14260 USA (e-mail: krishna.bhat@ieee.org; kwangoh@buffalo.edu).

D. C. Hopkins is with the Department of Electrical and Computer Engineering, North Carolina State University, Raleigh, NC 27695 USA (e-mail: d.hopkins@ieee.org).

Color versions of one or more of the figures in this paper are available online at http://ieeexplore.ieee.org.

Digital Object Identifier 10.1109/TIA.2012.2229681

I. INTRODUCTION

AN oil-immersed power transformer is used as a case study to show feasibility for a microelectromechanical systems (MEMS)-based gas sensor approach in high-voltage (HV) apparatus. Oil inside a transformer undergoes relatively rapid decomposition, depending on fault type or overload conditions [1]. The decomposition generates small amounts of gas molecules at high velocities and at relatively higher pressure and temperature than the surrounding oil [2]. The energy stored within the gas molecules can be compared with that of the surrounding oil as a function of quantity and time and then converted to a variable electrical output by using a MEMS sensor consisting of multiple microturbines centrally shafted to a microgenerator. The turbine generator model is set up within an encapsulated structure to be placed deep within the oil at close proximity to the transformer windings. Using multiple MEMS sensors within the transformer, it is possible to create a 3-D image of the transformer and analyze individual spots of degrading insulation and of overload conditions, depending on the amount of gas produced and oil displaced. The voltage outputs of the MEMS generators can be conditioned and transmitted wirelessly or through optical fiber to an external receiving unit, which aggregates multiple sensor data for spatial mapping.

II. GAS PRODUCTION

The gas is primarily produced by the chemical and physical decomposition of the oil and winding insulation due to inordinately HV gradients in the transformer. The quantity of gas produced can vary anywhere from a cubic centimeter to 2 m^3 [3]. Almost 70% of the gas generated during normal and fault conditions is comprised of hydrogen [4]–[9]. During extreme faults, the overall oil displacement reaches up to 5 m/s, and the corresponding volume of gas due to vaporization could reach up to 3.4 m^3. For the MEMS sensor, the areas of interest are low intensity faults, i.e., $\sim$2 kJ, followed by a pressure wave of $\sim$100 kPa. It has been shown that during a fault of energy 2 kJ, there is substantial gas production (hydrogen and

0093-9994/$31.00 © 2012 IEEE

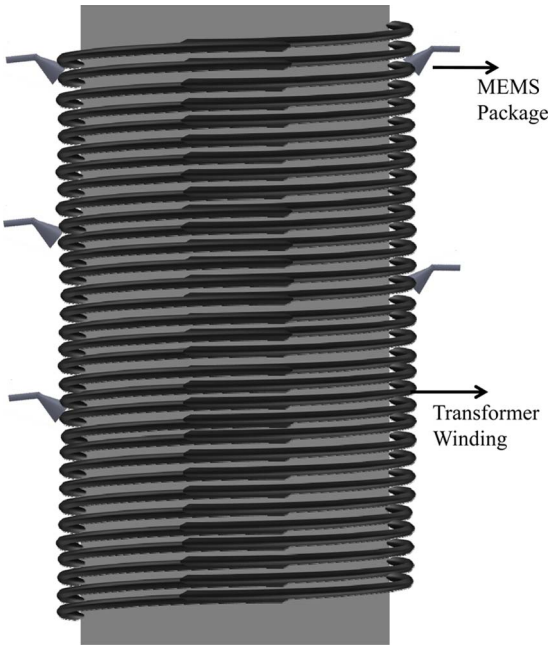

Fig. 1. Positioning of the MEMS device with span limited to few turns in transformer windings. Miniature size reduces field stress.

acetylene) [3]. The corresponding velocity of the gas bubbles can range between 0.1 and 0.5 m/s during minor fault conditions, depending on the type of oil and transformer in use [3]. The amount of gas produced drastically increases the risk of a transformer explosion. For very low intensity operation, it has been shown that, in certain insulating liquids, localized injection of electrical energy (1–20 nJ) creates gas bubbles of about micrometer size followed by a low-pressure wave [10]. The Rayleigh model relates the bubble lifetime (Δt) to the maximum bubble radius (R_m), density (ρ), and hydrostatic pressure (P), as shown in the following equation:

$$\Delta t = 1.83 R_m \sqrt{\frac{\rho}{P}}. \tag{1}$$

The bubble radius can be related to the injected energy (E) and Boltzmann's constant (k) using a similar thermodynamic model, as shown in the following equation:

$$R_m = k \left[\frac{E}{P}\right]^{\frac{1}{3}}. \tag{2}$$

Equations (1) and (2) are further used in Section III-B to relate gas bubble formation to the energy transfer.

III. Design and Workings of the Proposed MEMS Sensor

The positioning of the proposed MEMS sensor is shown in Fig. 1 The sensor is physically attached at multiple positions around the transformer-winding stack to maximize oil and gas bubble flow through the sensor. The advantage of using a MEMS-based sensor is to provide miniature features allowing it to span only one to two windings and be mounted on the windings. This presents a relatively low field gradient

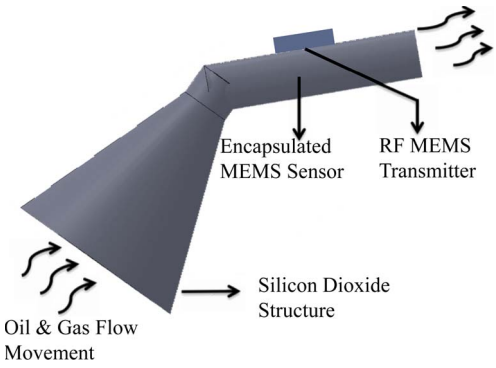

Fig. 2. Conceptual design and positioning of MEMS components to form the MEMS transducer, along with a data transmitter.

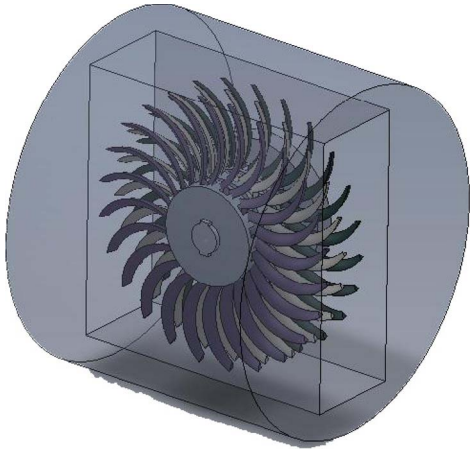

Fig. 3. MEMS turbine. Gas flow enters a graduated collection tube (not shown) and hydraulically drives a MEMS turbine.

in a very HV transformer. The MEMS encapsulate should have a closely matched permittivity to the operational ratings of the oil and winding insulation and should withstand high electrical and mechanical stresses. Materials, such as ceramics, silicon oxides, silicones, and parylene, are commonly used in microelectronics, which have high dielectric strengths and similar permittivity. Mechanical geometry also affects localized electric field distribution.

The sensor includes a collection tube, as shown in Fig. 2. The tube has a collection port of calculated size for gas entrance to provide a calibrated gas volume. The area of the port opening is dependent on fluid (oil) characteristics and changes depending on product application. The tube narrows and optimally concentrates the flow volume entering the turbine chamber.

A. MEMS Transducer: Turbine, Gearing, and Generator

The MEMS transducer section of the sensor has four stages to transfer hydraulic energy into an electrical signal: graduated collection tube (noted earlier), MEMS turbine (see Fig. 3), gearing, and generator (see Fig. 4). The MEMS turbine is the primary component of the transducer and transfers fluidic energy of the bubble flow into rotational energy. Gearing is used to increase shaft speed, which in turn drives a MEMS generator. The generator produces a proportional electrical output signal representing bubble generation by the stressed transformer windings.

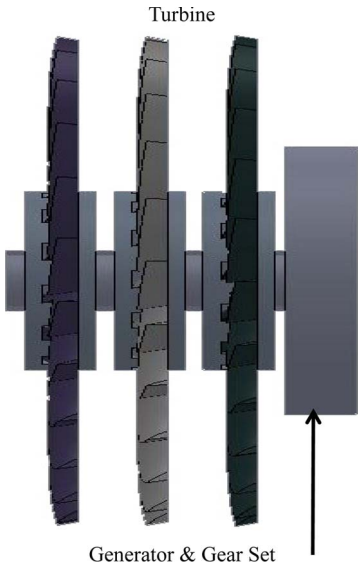

Fig. 4. MEMS turbine and generator arrangement. The turbine is geared to a generator, which produces an electrical signal proportional to gas flow.

B. Working Principle

The turbine works on the principle that the gas bubble present in oil has higher temperature, pressure, and velocity than the surrounding oil [11]. Hence, the gas bubble has a relative difference in energy to the surrounding oil flow [12]. When the combined gas and oil flow impinges on the MEMS turbine blades, the flow converts a portion of the energy into mechanical rotation of the turbine. The MEMS device is used to measure the relative difference in the gas parameters (pressure and velocity) during various working conditions. The formation of bubbles can be explained as a fluidic interface given by the Young–Laplace equation $\Delta P = \sigma((1/R_1) + (1/R_2))$ [13], where ΔP is the difference in pressure between the enclosed gases and surrounding fluid, σ is the surface tension acting on the bubble, and R_1 and R_2 are the radii of curvature of the bubble [$R_1, R_2 < R_m$, from (1) and (2)].

Studies and experiments have shown that it is difficult to obtain a generalized equation for the exact velocity and energy enclosed by a gas bubble [12]. The energy depends on various factors: bubble formation, physical and chemical properties of the surrounding fluid, characteristic flow at the fluid interface, net forces acting on the oil–gas interface, etc. The radiation and vaporization process accounts for the energy loss following a fault. This loss is usually represented as a percentage depending on the type of fluid and the required form of energy and is usually within 10%–70% of the total electrical energy[12]. However, the minimum work required to form a nucleus of gas within a homogeneous liquid can be determined and used as a minimum design point [12]. The work is given by

$$\Delta\Phi = \frac{4}{3}\pi R^3\left(P_O - P + P\ln\frac{P}{P^*}\right) + 4\pi R^2\sigma + KT\sum_i n_i \ln\frac{y_i}{y_i^*}. \tag{3}$$

The closest approximation for the total energy of a gas bubble flowing through a fluid can be compared with the energy involved in the fluid layer interface (oil–gas), as shown in the following equation [12]:

$$dE = dE_1 + dE_2 + dE_3$$
$$E = \int_0^x \left[\left(\frac{\phi}{1-\phi}\rho_f g x Q_g\right) + \left(\rho_g + \frac{\rho_f}{2}\right)\frac{v_f^2}{2\phi} + \frac{3\sigma}{R}\phi\right] dx. \tag{4}$$

The energy exchange from the fluid to the turbine occurs within the defined space at the intermolecular level, satisfying the energy conservation equations, such as mass, momentum, and energy, as shown in the following [14]:

$$\frac{\partial\rho}{\partial t} + \frac{\partial(\rho\bar{c}_j)}{\partial x_j} = 0 \tag{5}$$

$$\frac{\partial(\rho\bar{c}_i)}{\partial t} + \frac{\partial(\rho\bar{c}_i\bar{c}_j)}{\partial t} = -\frac{\partial\rho}{\partial x_i} + \frac{\partial\tau_{i_j}}{\partial t} + \rho\overline{F}_i \tag{6}$$

$$\frac{\partial\left(\rho e + \frac{1}{2}\rho\bar{c}^2\right)}{\partial t} + \frac{\partial\left[\rho\bar{c}_j\left(h + \frac{1}{2}\bar{c}^2\right)\right]}{\partial t} = \frac{\partial(\tau_{jk} - q_i)}{\partial x_j} + \rho\overline{F}_j\bar{c}_j. \tag{7}$$

The energy transfer from the windings to the oil is given by $\dot{E} = W \times H(t)$ [3], where $\dot{E}$ is a percentage of the total energy (E), W is the instantaneous power, and $H(t)$ is a function governing the energy transfer.

The combined mechanical output power (P) of the microturbine (percentage of W) following the transfer of energy from the gas bubble and oil flow, is given by Von Karman's equation [15]

$$P = 2M\omega$$
$$M = 0.31\pi\rho a^4\sqrt{v\omega^3}. \tag{8}$$

Equation (8) indicates that the power developed by the rotor proportionally depends on both the kinematic viscosity of the fluid (ν) and the angular velocity of the turbine blade (ω). However, in actuality, the angular velocity of the blade is inversely proportional to the kinematic viscosity, as indicated by Newtonian flow equation $\tau = \nu\rho\partial x/\partial t$, where τ is the stress acting on the fluid and ν and ρ are the respective dynamic viscosity and density of oil. As seen from the expression, for constant stress, the higher the viscosity, the lower the velocity. This reflects on (8), under which the power developed can be expressed as a function $f = \{\omega^{5/2}(\nu^{-1}), \nu^{1/2}\}$.

The final design characteristics of the sensor are dependent on the energy transfer efficiency of the gas bubble. This correlates with many application-specific factors and requires a standard computational approach to evaluating the well-understood transfer mechanism [12].

IV. Reverse Scaling

The working of a micropump can be closely related to the reverse working of a MEMS transducer. Microrotary pumps, such as those shown in Fig. 5, with diameters of 2.3 mm have been designed for pumping fluids at the rate of 2.1 ml/min, which is achieved at a pressure of 1.19 kPa at 211 r/min [16].

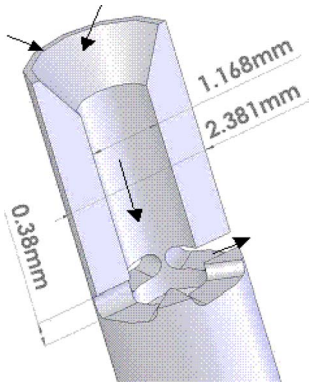

Fig. 5. Double-disk viscous micropump developed at the University of Utah, Mechanical Engineering, March 2005 [16].

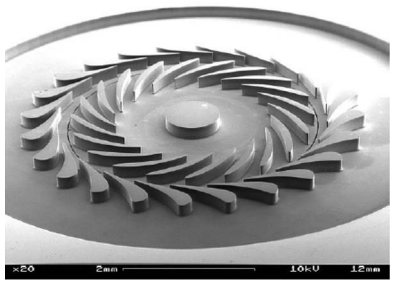

Fig. 6. Radial flow turbine with a 4-mm rotor diameter used for power generation through hydrogen combustion. Designed by the Gas Turbine Laboratory, Massachusetts Institute of Technology (MIT), Cambridge, 2003 [18].

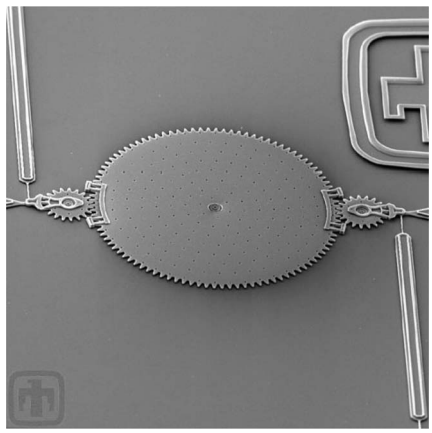

Fig. 7. Microgearing demonstrated by Sandia National Laboratories, Sandia ST&E Microsystems and Gears [19].

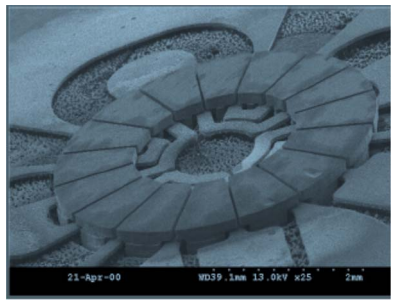

Fig. 8. Magnetic motor/generator with a 4-mm diameter used in the MIT Gas Turbine Project [18].

An equivalent reverse function of the pump with relevant or reduced design parameters can produce electrical signals within the relative range needed for this application. The construction of a microgenerator varies from that of a micropump, with appropriate changes to the turbine blade design and channeling of fluid flow to preserve blade efficiency.

With the present limited options to show an actual design of a fluidic turbine specifically geared for power generation, it is necessary to relate design changes to existing micropumps. Flow-rate measurements above 5×10^{-5} m^3/s for liquids and 5×10^{-4} m^3/s for gases have been shown to be achievable, using movable parts, specifically turbines [17]. Further research and demonstration would optimize design of impeller blades and flow interface to optimize mechanical power generation. MEMS combustion turbines exist for power generation. One such turbine shown in Fig. 6 is used for power generation through microrotary components and demonstrates the feature sizes required for the MEMS transducer. As explained in Section IV, the MEMS sensor attached to the transformer windings is used to collect the combined flow of gas and oil during the degradation of insulation.

The size of the bubble and the duration for which it maintains its physical size and shape is primarily explained by (1) and (2). The energy from the transformer windings is used to form gas bubbles, as mentioned by (3). As indicated, the size, time, and energy of the gas bubble are interrelated and directly proportional to the energy generated by the winding during abnormal conditions. The oil and gas close to the winding are at a relatively higher energy level, as represented in (4). The fluid flow then carries the mass, energy, and momentum [specific to (5)–(7)] over a distance for the specific duration of time (Δt), dependent on the type, time period, and intensity of transferred energy. Equations (1)–(7) provide the design requirements for feature size of the impellers and desired rotational speed. Furthermore, the series turbine arrangement (see Fig. 4) can improve energy transfer and uses a lower rpm.

Blanchard *et al.* [16] (see Fig. 5) reported a pumping capacity of 2.1 ml/min with a head pressure of 1.19 kPa at 211 r/min. From the discussion in Section II, the overall gas flow available to the MEMS sensor can be up to 0.5 m/s and would be accompanied with a pressure wave up to 100 kPa during abnormal transformer fault operation. The feature dimensions cited here for MEMS devices are within the range needed to produce the proposed MEMS sensor.

A centrally shafted microgenerator is used to produce an electrical signal proportional to the gas flow. The microgenerators are normally designed to operate at relatively higher rpm ($>$ 1000 r/min). Some of the present manufactured gears and low-power permanent magnet generators are shown in Figs. 7 and 8.

V. Design Summary

Sustained transfer of energy is the critical step in the sensing of abnormal changes in the transformer. Uncontrolled transient fluidic flow measurement in open oil systems is recognized as a challenging field of research. Combined with the possibility of relatively large fluid flows, the turbine sensing method is preferred over most other MEMS flow-rate measurement

techniques [17]. The close proximity of the sensor to the winding directly allows the fluid (gas and oil) to pass through the sensor at the point of highest energy generation. With the large volume of fluid (as compared to the size of the turbine) passing through the sensor, the energy and momentum are transferred to the fluid turbine blades. The blades are the most important component of the sensor and are optimally designed to operate at low energy levels and rpm. Furthermore, the turbine blade design should be specific to the application. For example, power transformers $>$ 200 MVA operate at very high potentials, and the possible transfer of energy during abnormal conditions can be higher compared with that of lower power pole transformers. Therefore, the turbine design of a MEMS sensor used in a power transformer can be relatively larger in size to match the magnitude of energy transferred.

The generator design follows a similar rule to that of the turbine. However, the manufacturing process can be more streamlined by using permanent magnet dc motors/generator set. This helps in providing a quick response output to the turbine torque and also eliminates field currents. The size of the generator would directly correspond to that of the turbine owing to the transfer of energy from the winding.

The output of the generator can be fed to an RF MEMS transmitter, which produces an RF signal in direct relation to that of the electrical dc output. The advantage of selecting the RF is the uniformity of oil as a transmission medium. Similar to the selection of electromechanical components for the RF device, the designated RF transmission frequency of a MEMS sensor has to be selected considering the RF interference from partial discharge and HV transients.

VI. Summary

This paper has discussed the feasibility of using MEMS sensors to detect energy levels in gas generation from several fault scenarios occurring in oil-filled apparatus, with specific focus on HV power transformers. Specific ranges of energy defined through mass, volume, pressure, etc., of the generated gas has been identified using an extensive review of the literature. Specific designs of existing MEMS sensors that have related functionality have been identified, and critical aspects of their designs have been discussed along with specific energy ranges of their operation. Together, feasibility is shown and an approach outlined for development of MEMS-based sensing of faults in HV apparatus.

Through extensive review of the literature, the characteristics and energy levels of gas liberated during faults have been determined. The energy is quantified in terms of mass, pressure, and velocity. For example, the quantity of gas produced can vary anywhere from a cubic centimeter to 2 m^3 with almost 70% as hydrogen, which sets a lower limit on mass. For low intensity faults of $\sim$2 kJ, a pressure wave of $\sim$100 kPa has been measured with a corresponding velocity of the gas bubbles that can range between 0.1 and 0.5 m/s. This information is used with a specific Rayleigh equation to characterize the size and energy of the range of gas bubbles to be detected. A sequence of equations has been developed to determine the minimum energy transfer from the gas to a MEMS-based impeller, which also identifies critical design parameters. A step-by-step procedure is given for using the equations.

A set of MEMS devices has been identified to show feasibility of coupling an electrical generator to the impeller(s) through MEMS gearing. From the discussion in Section II, the overall gas flow available to the MEMS sensor can be up to 0.5 m/s and would be accompanied with a pressure wave up to 100 kPa during abnormal transformer fault operation. The feature dimensions cited for MEMS devices in Section V are within the range needed to produce the proposed MEMS sensor.

References

[1] Y. C. Liang and J. L. Liu, "Power transformer based diagnosis using SOM based RBF neural networks," in *Proc. 5th Int. Conf. Mach. Learn. Cybern.*, Dalian, China, Aug. 2006, pp. 3140–3143.

[2] F. Jomni, F. Aitken, and A. Denat, "Investigation of the behaviour of microscopic bubbles in insulating liquids: Transition from inertial regime to the viscous one," in *Proc. 14th ICDL*, Graz, Austria, Jul. 12, 2002, pp. 194–198.

[3] S. Muller, M. P. Boiarciuc, and G. Perigaud, "Protection of oil-filled transformer against explosion: Numerical simulations on a 200 MVA transformer," in *Proc. IEEE Bucharest Power Tech Conf.*, Bucharest, Romania, Jun. 28–Jul. 2, 2009, pp. 1–8.

[4] Y. Zhang, X. Ding, Y. Liu, and P. J. Griffin, "An artificial neural network approach to transformer fault diagnosis," *IEEE Trans. Power Del.*, vol. 11, no. 4, pp. 1836–1841, Oct. 1996.

[5] J. L. Guardado, J. L. Naredo, P. Moreno, and C. R. Fuerte, "A comparative study of neural network efficiency in power transformers diagnosis using dissolved gas analysis," *IEEE Trans. Power Del.*, vol. 16, no. 4, pp. 643–647, Oct. 2001.

[6] J. J. Dukarm, "Transformer oil diagnosis using fuzzy logic and neural networks," in *Proc. Can. Conf. Elect. Comput. Eng.*, 1993, vol. 1, pp. 329–332.

[7] C. E. Lin, J. M. Ling, and C. L. Huang, "An expert system for transformer fault diagnosis using dissolved gas analysis," *IEEE Trans. Power Del.*, vol. 8, no. 1, pp. 231–238, Jan. 1993.

[8] W. Xu, D. Wang, Z. Zhou, and H. e Chen, "Fault diagnosis of power transformers: Application of fuzzy set theory, expert systems and artificial neural networks," in *Proc. Inst. Elect. Eng.—Sci. Meas. Technol.*, Jan. 1997, vol. 144, no. 1, pp. 39–44.

[9] Y. C. Huang, H.-T. Yang, and C.-L. Huang, "Developing a new transformer fault diagnosis system through evolutionary fuzzy logic," *IEEE Trans. Power Del.*, vol. 12, no. 2, pp. 761–767, Apr. 1997.

[10] F. Jomni, F. Aitken, and A. Denat, "Dynamics of microscopic bubbles generated by a corona discharge in insulating liquids," *J. Electrostat.*, vol. 47, no. 1/2, pp. 49–59, Jun. 1999.

[11] S. Prigent, M. Darcherif, A.-M. Lehnert, P. Magnier, J. Wild, and D. Scheurer, "Comparison of the SERGI developed magneto-thermo-hydrodynamic model results with measurements made on a 160 KVA transformer," in *Proc. IEEE Section Mexico, Acapulco*, Jul. 9–14, 2000, IEEE Ref: rpijp01a, dated May 29, 2000.

[12] N. P. Cheremisinoff, Ed., "Gas–Liquid Flows," in *Encyclopedia of Fluid Mechanics*. Houston, TX: Gulf, pp. 130–140, Library of Congress Cataloging-in-Publication Data.

[13] J. A. Pelesko and D. H. Bernstein, *Modeling MEMS and NEMS*. Boca Raton, FL: CRC Press, pp. 76–77.

[14] W. G. Vincenti and C. H. Kruger, Jr., *Intro to Physical Gas Dynamics*. New York: Wiley, 1965, pp. 316–327.

[15] J. Kao, J. Warren, and J. Xu, "A bubble powered micro-rotor: Manufacturing, assembly and characterization," in *Proc. ASME Int. Mech. Eng. Congr. Exp.*, Chicago, IL, Nov. 5–10, 2006, pp. 611–615.

[16] D. Blanchard, P. Ligrani, and B. Gale, "Single-disk and double-disk viscous micropumps," *Sens. Actuators A, Phys.*, vol. 122, no. 1, pp. 149–158, Jul. 29, 2005.

[17] S. Colin, *Microfluidics*. London, U.K.: ISTE, 2010, pp. 307–310.

[18] A. H. Epstein, "Millimeter-scale, MEMS gas turbine engines," in *Proc. ASME Turbo Expo, Gas Turbine Lab., Power Land, Sea, Air*, Atlanta, GA, Jun. 16–19, 2003, pp. 669–696.

[19] J. J. Sniegowski, "Chemical–mechanical polishing: Enhancing the manufacturability of MEMS," in *Proc. SPIE—Micromach. Microfabrication Process Technol. II*, Sep. 23, 1996, vol. 2879, p. 104, doi:10.1117/12.251237.

Krishna Prasad Bhat (S'09–M'12) received the M.S. degree in electrical engineering from the University at Buffalo, State University of New York, Buffalo, in 2009.

He is currently a Research Engineer at Ford Motor Company working on automotive traction inverter semiconductor devices. His research interests include monitoring high-energy transient faults in power transformers.

Kwang W. Oh received the Bachelor's degree in physics from Chonbuk National University, Jeonju, Korea, in 1995 and the M.S. and Ph.D. degrees in electrical and computer engineering from the University of Cincinnati, Cincinnati, OH, in 1997 and 2001, respectively.

He is an Associate Professor with the University at Buffalo, State University of New York (SUNY at Buffalo), Buffalo, where he leads the Sensors and MicroActuators Learning Laboratory (SMALL) (small.buffalo.edu or MicroTAS.org). Prior to joining SUNY at Buffalo, he was with Samsung Advanced Institute of Technology, Korea, where he developed micro-polymerase-chain-reaction and lab-on-chip platforms for clinical diagnostics. He has authored 85 technical papers and three book chapters. He is the holder of 24 patents. His current research focuses on droplet-based microfluidics, microfluidic networks, 3-D cell culture platforms, microvalves and actuators, and microfluidic applications for terahertz spectroscopy, platelet aggregation, and metamaterials. His research has been supported by the Korea Institute of Science and Technology, by the National Science Foundation, and by the New York State Office of Science, Technology and Academic Research.

Douglas C. Hopkins (M'73–SM'92) received the B.S. and M.S. degrees from the State University of New York at Buffalo (UB), Buffalo, and the Ph.D. degree from Virginia Polytechnic Institute and State University, Blacksburg, where his primary study was in megahertz-frequency power conversion using high-density packaging techniques.

Prior to his postdoctoral study, he worked with the corporate research and development centers of General Electric and Carrier. After his postdoctoral work, he held appointments at Auburn University and Binghamton University and returned to UB, where he became the Director of the Electronic Power and Energy Research Laboratory and the Assistant Director of the Electronic Packaging Laboratory. In 2011, he became the Director of the laboratory for "Packaging Research in Electronic Energy Systems" (part of the NSF-ERC FREEDM Center) and a Professor in electrical and computer engineering with North Carolina State University, Raleigh, where he is conducting research in packaging of kiloampere and kilovoltage power electronic systems. He held Visiting Faculty Fellowships at the Lawrence Livermore National Laboratory, U.S. Army, NASA, and Ohio Space Institute. He founded two SBIR-funded companies. He has authored over 100 journal and conference publications.

Dr. Hopkins is a Fellow of the International Microelectronics and Packaging Society.